

Active substrate termination of discrete and monolithic bidirectional GaN HEMTs in a T-type inverter

Carsten Kuring¹, Yannic Lange¹, Xiaomeng Geng¹, Oliver Hilt², Mihaela Wolf², Joachim Würfl² and Sibylle Dieckerhoff¹

¹ TECHNISCHE UNIVERSITÄT BERLIN
Einsteinufer 19
Berlin, Germany

² FERDINAND-BRAUN-INSTITUT
LEIBNIZ-INSTITUT FÜR HÖCHSTFREQUENZTECHNIK
Gustav-Kirchhoff-Str.4
Berlin, Germany
Tel.: +49 30 314 23404
Fax: +49 30 314 25526
E-Mail: carsten.kuring@tu-berlin.de
¹ URL: <https://www.pe.tu-berlin.de>
² URL: <https://www.fbh-berlin.de>

Keywords

«Gallium Nitride (GaN)», HEMT, Monolithic power integration, Multi-level inverters, DC-AC converter

Abstract

Monolithically integrated lateral Gallium-nitride bidirectional transistors can achieve symmetric conduction and blocking capability at a reduced on-state resistance compared to their discrete counterparts. An actively switched substrate effectively prevents back-gating effects in normally-off GaN-on-Si bidirectional transistors and enables symmetrical loss-minimized switching and on-state characteristics.

Introduction

Power electronic topologies such as the multi-level T-type inverter, matrix-inverter and current-sourced inverters require power semiconductor switches featuring bidirectional voltage-blocking capability. Lateral chip-design of Gallium-nitride high-electron-mobility transistors (GaN HEMTs) enables monolithic integration of several power transistors into a single chip. Monolithically integrated bidirectional GaN HEMTs allow to minimize the parasitic stray inductance in fast switching GaN-based power electronics. Bidirectional GaN HEMTs implementing a common drift region for both blocking voltage polarities can achieve an almost 50% lower on-resistance (R_{ON}) compared to discrete bidirectional switches [1, 2, 3]. Considering power electronic topologies such as the multilevel T-type inverter significantly reduced conduction losses are expected as long as stable bidirectional device characteristics are maintained and device degradation is prevented.

Normally-off GaN HEMTs fabricated on a conductive silicon (Si) substrate are prone to back-gating effects leading into current collapse and degraded on-state characteristics depending on the applied substrate bias. Therefore, an appropriate substrate termination is essential to ensure efficient and symmetric bidirectional switched operation. This paper discusses different implementation schemes of bidirectional GaN transistors in Sec. 1 including a discrete GaN-based bidirectional switch specifically designed to emulate substrate coupling-effects occurring in monolithic bidirectional GaN HEMTs. Sec. 2 demonstrates the degradation of static device characteristics due to negative substrate bias. Different substrate termination schemes suitable for switched operation are derived in Sec. 3. An experimental validation regarding switching characteristics and transient R_{ON} under hard- and soft switching conditions in double-pulse switching tests are presented in Sec. 4. Selected substrate termination schemes are further evaluated concerning converter efficiency and device temperature in continuous DC/DC buck operation. According to the obtained measurement results, an actively switched substrate enables efficient bidirectional operation of bidirectional GaN HEMTs.

1 Implementation of discrete and monolithic bidirectional GaN HEMTs

Bidirectional blocking capability can be implemented in either common drain (Fig. 1a) or common source configuration (Fig. 1b) [4, 5, 6]. In order to prevent device degradation in terms of reduced saturation current and increased R_{ON} induced by back-gating effect, the conductive Si-substrate in conventional unidirectional normally-off GaN HEMTs is shorted to the source node [7, 8]. This paradigm is satisfied for discrete bidirectional transistors with separate bulk node (Fig. 1a) as well as monolithic bidirectional transistors with common source and common bulk node (Fig. 1b). However, it is not feasible for monolithic bidirectional HEMTs with common drift region, which can achieve a significantly lower R_{ON} similar to a single unidirectional Gan HEMT as the same drift-region l_{GaGb} is utilized for positive as well as negative blocking voltage polarity (Fig. 1c) [1, 2, 3, 9, 10]. In case of the monolithic bidirectional HEMT presented in [2] saturation current degradation and increased R_{ON} by back-gating effects have been observed. The substrate must be terminated to the one of both source nodes S_a and S_b with the lower potential to avoid the observed back-gating effects. Since the applied blocking voltage polarity changes in device operation, switching of the backside termination between S_a and S_b may be feasible to prevent back-gating and enable minimized bidirectional conduction losses (TABLE I).

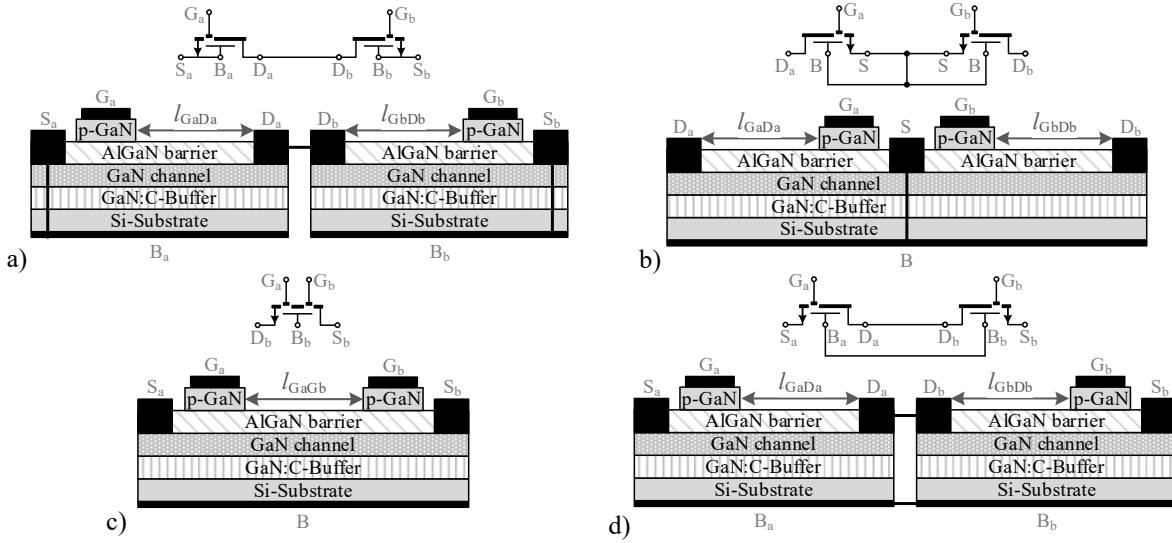


Fig. 1: Bidirectional switch implementation using lateral GaN HEMTs: (a) discrete switch in common drain configuration, (b) monolithic switch in common source configuration, (c) monolithic switch with common drift region and common substrate and (d) discrete switch with common bulk and common drain node

In this paper a monolithic bidirectional HEMT with common drift region is emulated using two commercially available discrete GaN-on-Si HEMTs with shorted bulk and drain terminals (Fig. 1d). This configuration reproduces substrate coupling and biasing effects of a bidirectional transistor with common substrate and common drift-region, while the R_{ON} is still doubled.

TABLE I. Optimum bulk termination scheme of a bidirectional GaN HEMT

Operation direction		Forward	Reverse
Off-state blocking voltage	$V_{SbSa,off}$	> 0 V	< 0 V
Operation mode of	S_a	actively switched	acting as Drain
	G_a		continuously turned on
	S_b	acting as Drain	actively switched
	G_b	continuously turned on	
Optimum bulk termination		bulk terminated to S_a	bulk terminated to S_b

2 Static device characteristics

The susceptibility to current collapse induced by back-gating is demonstrated by means of the static device characteristics extracted from pulsed IV measurements covering a single unidirectional GaN HEMT GS66508P as well as the emulated monolithic bidirectional (Fig. 1d).

A shorted termination of the substrate to source ($V_{BS}=0$ V) is recommended by the device manufacturers to achieve ‘best device performance’ [7, 8]. In case of the bidirectional transistor the second gate G_b is biased at $V_{GbSb}=6$ V. In this configuration both, the unidirectional and bidirectional GaN HEMT exhibit

a good controllability by means of the gate-source bias. Thereby asymmetrical saturation currents of $I_{\text{Sa},\text{max},\text{Q1}}=136 \text{ A}$ and $|I_{\text{Sa},\text{max},\text{Q3}}|=|-106 \text{ A}|$ are observed for the bidirectional transistor compared to $I_{\text{D},\text{max},\text{Q1}}=102 \text{ A}$ in the unidirectional reference GaN HEMT (Fig. 2a vs. b). Despite the series interconnection of two separate unidirectional GaN HEMTs in the bidirectional transistor, the static R_{ON} is only increased from $R_{\text{on}}=50.6 \text{ m}\Omega$ to $R_{\text{on}}=89.6 \text{ m}\Omega$ (Fig. 2c). The observed deviations in device characteristics are related to a reduced threshold voltage in the bidirectional transistor (Fig. 2d) possibly caused by device degradation induced by the bulk-source voltage stress applied during the measurements.

Assuming an increasingly negative bulk-source bias $V_{\text{BS}}<0 \text{ V}$ the two-dimensional electron gas (2DEG) is depleted causing lower saturation currents and increased R_{ON} (Fig. 2e, f) in both, 1st- and 3rd-quadrant operation. At the lowest considered bulk-source bias $V_{\text{BS,min}}=-300 \text{ V}$ both devices are effectively blocking even at the highest considered gate-source bias $V_{\text{GS,max}}=6 \text{ V}$. For positive bulk-source bias $V_{\text{BS}}>0 \text{ V}$ the output characteristic remains almost unaffected. In conclusion, the bulk acts as additional terminal controlling the GaN HEMT. In order to achieve a low R_{ON} and therefore efficient in-circuit switched operation the applied substrate termination schemes must prevent a negative bulk-source bias.

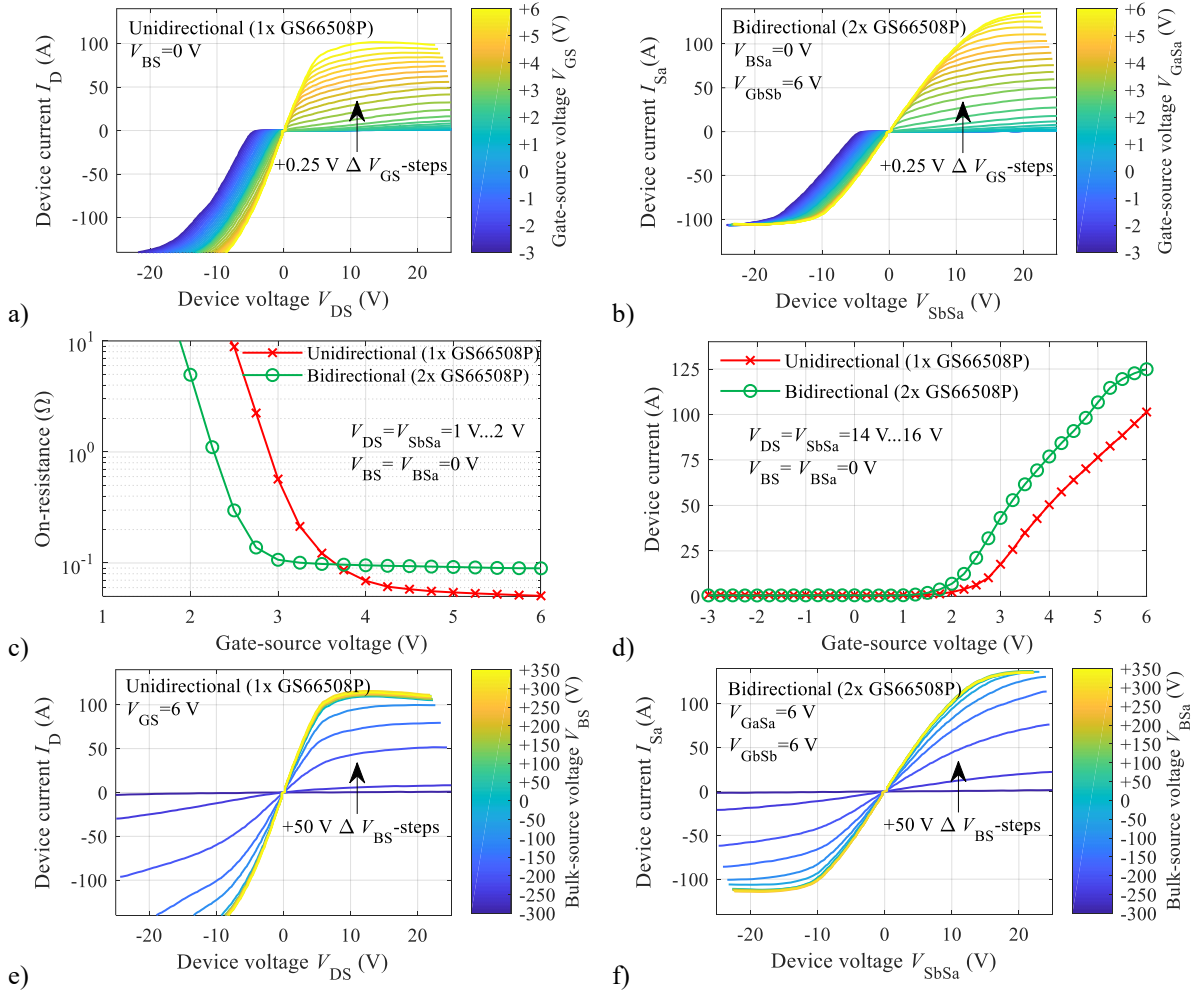


Fig. 2: Static IV characteristics of a unidirectional GaN HEMT (1x GS66508P) vs. an emulated bidirectional GaN HEMT (2x GS66508P) at (a...d) varied gate-source bias and (e...f) varied bulk-source bias

3 Substrate termination schemes

According to the obtained pulsed IV-measurement results a proper substrate termination is mandatory to ensure low on-state losses in monolithic bidirectional GaN HEMTs. Different substrate termination schemes have been proposed before [11, 12, 13]. However, measurement results validating the overall functionality especially concerning an actively switched substrate have not been published so far. Similar to [2] this paper covers two different fixed substrate terminations I and II, where the bulk is permanently shorted to one of both source nodes S_a, S_b (Fig. 3a, b). Assuming one of these substrate terminations, the other one will inevitably occur as soon as the blocking voltage polarity of the bidirectional

HEMT changes (TABLE I). According to the blocking voltage polarity the configurations I and II would result in asymmetric on-state characteristics of the bidirectional GaN HEMT as they correspond to a source- and drain-connected substrate of a unidirectional GaN HEMT. A floating substrate (Fig. 3c) can achieve symmetric, but still degraded on-state characteristics as previously demonstrated for a monolithic bidirectional GaN HEMT [2]. A self-managed or semi-floating substrate by means of diodes D_I , D_{II} (Fig. 3d, e) is proposed in [11, 12, 13] and experimentally evaluated in this paper as well. Both diode-based substrate termination schemes require anti-serial diode configuration to maintain bidirectional blocking capability of the bidirectional switch. Depending on the specific diode configuration IV and V the substrate bias is limited to negative values $V_{BSx} < 0$ V and positive values $V_{BSx} > 0$ V, respectively. Discrete high-voltage PiN-diodes D_I , D_{II} with small parasitic device capacitance are employed minimizing the additional parasitic switching node capacitance in the targeted T-type inverter (TABLE II). An actively switched substrate VI is proposed in [11, 12, 13, 2] and is herein implemented by means of discrete unidirectional GaN HEMTs T_I , T_{II} (Fig. 3f, TABLE II). The substrate switches are connected in common-source configuration enabling a dynamic termination of the bulk node according to the blocking voltage polarity of the bidirectional HEMT. This circuit design is especially suitable for future monolithic integration of the bidirectional transistor together with the active substrate switches on a common conductive Si-substrate as all four incorporated transistors share the same bulk potential. In this study, substrate termination scheme VIa, where T_I is in on-state and T_{II} in off-state is – apart from the $R_{ON}=450\text{ m}\Omega$ of T_I – electrically equivalent to configuration I. Substrate termination scheme VIb, where both transistors T_I , T_{II} are in off-state, is electrically equivalent to configuration IV.

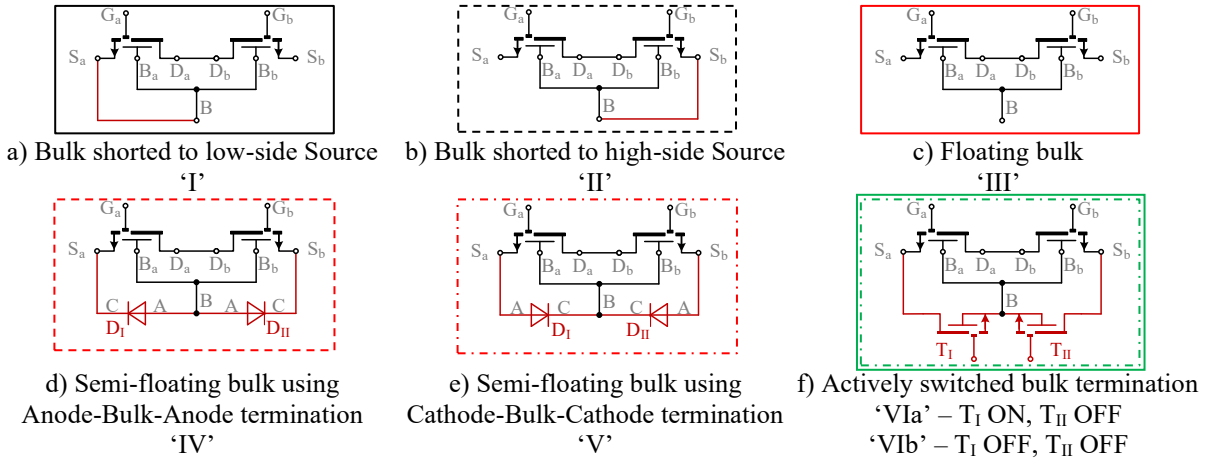


Fig. 3: Investigated fixed (a, b), (semi-) floating active (c...e) and active (f) substrate termination schemes

4 Switching characteristics in a T-type inverter

4.1 Test setup

The switching characteristics of the emulated bidirectional transistor T_2 formed by the unidirectional HEMTs T_{2a} and T_{2b} are investigated at DC-link voltages up to $V_{DC}=500$ V in a T-type inverter providing three output voltage levels $[-0.5 \cdot V_{DC}, 0\text{ V}, +0.5 \cdot V_{DC}]$. The T-type PCB-layout implements a vertical commutation loop design enabling minimum parasitic stray inductances by magnetic flux compensation. The impact of six different substrate termination schemes (Fig. 3) on the switching transients, voltage slew rates, switching losses and dynamic R_{ON} is studied. The transient on-state voltage is extracted by an actively controlled clamping circuit enabling calculation of the R_{ON} is calculated by means of the load current [14]. The power transistors as well as substrate switches are implemented by commercial discrete GaN-on-Si HEMTs (Fig. 4, TABLE II).

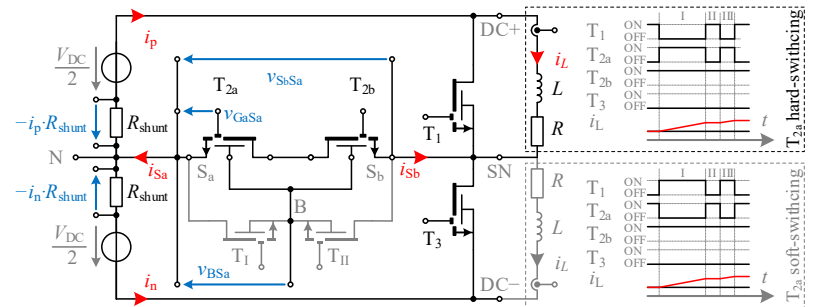


Fig. 4: Circuit diagram and control schemes of the emulated bidirectional GaN HEMT T_2 with active substrate termination in the T-type inverter

In hard-switched double-pulse tests of the bidirectional transistor T_2 , the unidirectional GaN HEMTs T_{2a} and T_1 are operated in 1st-quadrant hard-switching and 3rd-quadrant zero-voltage-switching (ZVS) free-wheeling mode, respectively. Vice versa, soft-switching and 3rd-quadrant ZVS free-wheeling mode of the bidirectional transistor T_2 is achieved by reconnecting the load inductor and adjusting the control signals where T_1 is now operated in hard-switched mode (Fig. 4). Transistors T_{2b} and T_3 are held in continuous on- and off-state respectively. In configuration VIa the substrate B is switched to source S_a by continuous on-state of T_1 while T_{II} remains turned off.

TABLE II: Semiconductor devices and gate configuration

Device / Parameter		Rating / value
GaN HEMT	T_1, T_3	GS66508B, 650 V, 50 mΩ
GaN HEMT	T_{2a}, T_{2b}	GS66508P, 650 V, 50 mΩ
GaN HEMT	T_1, T_{II}	GS-065-004-1-L, 650 V, 450 mΩ
Diodes	D_I, D_{II}	MA4P7470F-1072T, 800 V, 0.7 pF, 0.8 Ω
Gate drive voltages	$V_{G,\text{on}} / V_{G,\text{off}}$	+6.0 V / -2.0 V
Gate resistors	$R_{G,\text{on}} / R_{G,\text{off}}$	20 Ω / 10 Ω

4.2 Hard-switching characteristics in double-pulse test

In hard-switched operation turn-on and turn-off switching speeds significantly depend on the implemented substrate termination scheme. At moderate load currents $I_L < 8$ A, a floating (III) or semi-floating substrate (IV, V, VIb) leads to faster turn-off transitions including higher voltage slew rates and shorter current fall times (Fig. 5a and Fig. 6a). In contrast, at higher load currents $I_L > 12$ A either a permanently shorted (I) or actively switched substrate termination (VIa) results in higher turn-off voltage slew rates. In consequence, minimum turn-off losses can be achieved for a floating or semi-substrate in light-load conditions while a termination of the substrate to source S_a (I, VIa) yields into reduced switching losses at higher load currents (Fig. 6b). This effect may be further addressed and exploited by the proposed actively switched substrate VIa and VIb which differ only by the switching state of the substrate switches T_1 and T_{II} (Fig. 3f). Note that the load current at which the terminated (VIa) and semi-floating substrate (VIb) achieve similar turn-off switching losses slightly decreases from 11.56 A at $V_{DC}=300$ V to 10.52 A at $V_{DC}=500$ V due to non-linear voltage-dependent parasitic device capacitances. In substrate termination schemes II...V and VIb, where significant gradients of the substrate bias occur during turn-off transitions (Fig. 5a and b, left), the maximum turn-off voltage slew rate is limited to approx. +20 V/ns (Fig. 6a) due to device-internal substrate coupling effects.

The hard-switched turn-on transition is strongly affected by the applied substrate termination as well. Floating and semi-floating substrate configurations II-V and VIb result in slower turn-on transitions

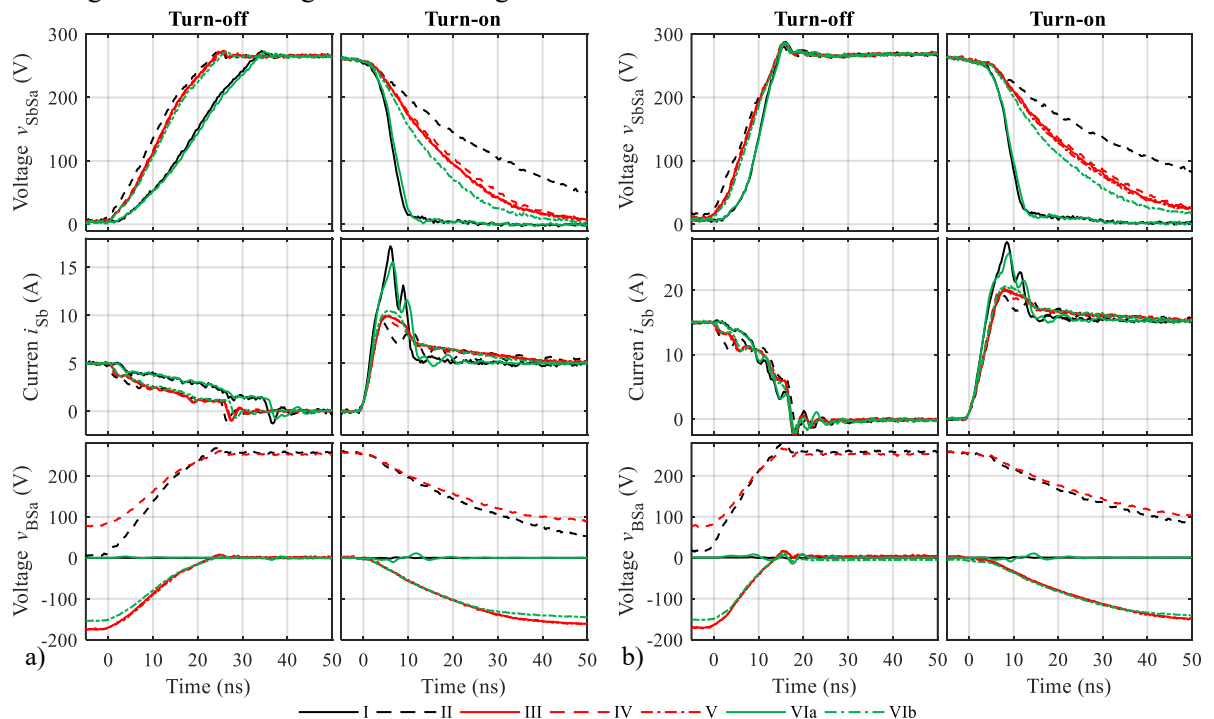


Fig. 5: Transients in hard-switched double-pulse test at load currents of (a) $I_L=5$ A and (b) $I_L=15$ A, $V_{DC}=500$ V

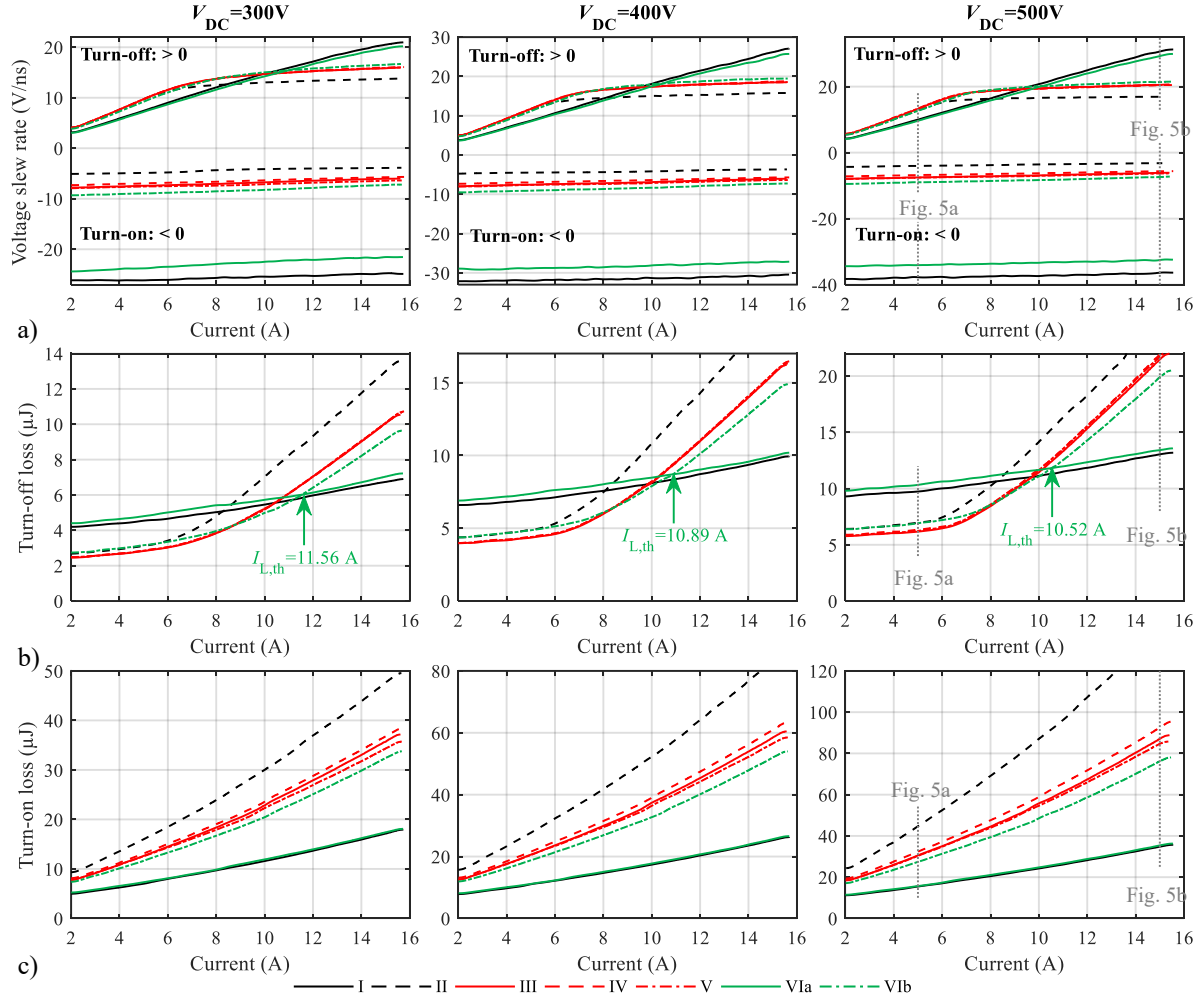


Fig. 6: Impact of the substrate termination on the (a) voltage slew rates (20%-80%), (b) turn-off and (c) turn-on switching losses

(Fig. 5a, b right) and severely increased turn-on losses (Fig. 6c). This effect occurs regardless of the substrate bias voltage prior turn-on (II, IV: $v_{BSa} \approx V_{DC}/2$ vs. III, V, VIb: $v_{BSa} \approx 0$ V), although device degradation in static measurements is limited to negative bulk-source bias (Sec. 2). However, a similar negative bulk-source voltage slew rate $d v_{BSa} / d t < 0$ is observed in all (semi-) floating substrate configurations (II-V, VIb). Despite the different substrate bias prior turn-on the bulk-source voltage drops by a similar magnitude during the hard-switched turn-on process for all the (semi-) floating substrate configurations (II-V, VIb). This is directly correlated to similar displacement currents charging and discharging the transistor's parasitic bulk capacitance. During GaN-on-Si device switching parasitic displacement currents aggravate short time charge trapping due to the continuous re-organization of the electron-hole equilibrium inside the GaN-based buffer and strain adaption layers of the transistor. Such semiconductor layer stack can be considered as an RC network with multiple time constants [15]. Partial depletion of the 2DEG and the observed slow turn-on process is a result of such dispersion phenomena (Fig. 6c). A fast and therefore loss-reduced turn-on transition is only achieved when the substrate is terminated to the low-side source S_a (Fig. 5, I and VIa). Additional parasitic device capacitances introduced by the active substrate switches (VIa) lead to marginally lower voltage slew rates as well as marginally increased switching losses in comparison to a permanently shorted substrate I. Considering the dominance of turn-on losses on the overall switching losses, an actively terminated substrate is mandatory to achieve loss-minimized hard-switched operation in bidirectional HEMTs. Consequently, subsequent dynamic R_{ON} measurements in double-pulse mode are limited to a comparison of the shorted substrate I with the switched substrate termination VIa.

The transient R_{ON} measurements of the bidirectional GaN HEMT in configuration I and VIa demonstrate a notable dynamic R_{ON} -increase when the R_{ON} before and after the blocking period are compared (Fig. 7a, $t < -1.1 \mu\text{s}$ vs. $t > 0.15 \mu\text{s}$). The average R_{ON} before blocking achieves a minimum value at

$V_{DC}=400$ V while lower as well as higher DC-link voltages result in a slightly increased R_{ON} (Fig. 7a, b) as reported in [16]. In contrast the dynamic R_{ON} -increase is triggered by the maximum field strength during blocking stress [17] and becomes more extensive at higher DC-link-voltage and load current (Fig. 7c, dashed vs. dot plot lines). The actively switched substrate termination VIa achieves a similar or even marginally lower R_{ON} compared to the reference short circuit I (Fig. 7, black vs. green plot lines) which is in general agreement with [2].

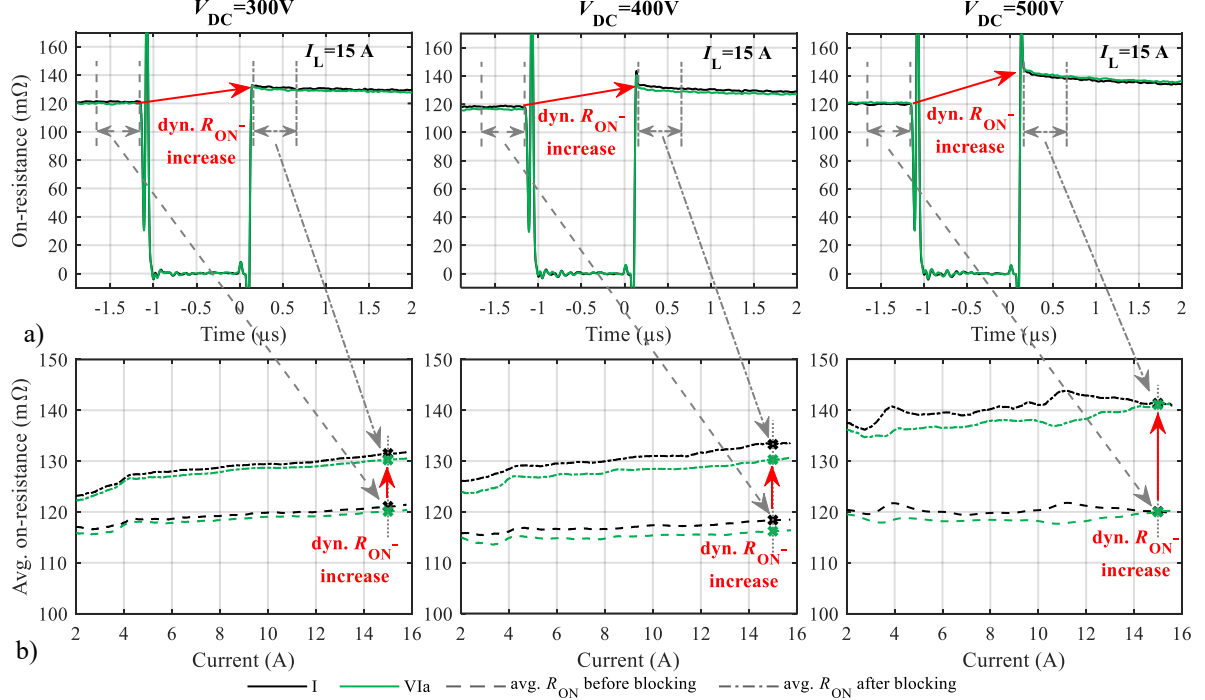


Fig. 7: Impact of the substrate termination on the (a) transient R_{ON} and (b) comparison of the R_{ON} before blocking vs. after blocking stress under hard-switched conditions. Note that the transistor off-state drain bias is $V_{DC}/2$.

4.3 Soft-switching characteristics in double-pulse test

In soft-switching conditions the emulated bidirectional GaN HEMT T₂ is operated in 3rd-quadrant reverse conduction mode achieving ZVS while the actively switched unidirectional GaN HEMT T₁ operated under hard-switched conditions. In consequence the impact of the employed substrate termination is much less pronounced, and the transient waveforms are inverted in comparison to the previous hard-switched characterization measurements.

In general, higher load currents result in shorter voltage fall-times during turn-on, as the charges in the parasitic switching node capacitance are displaced faster (Fig. 8a vs. b). The turn-off voltage slew rates decreases with the load current due to a longer current commutation. Non-linear voltage-dependent parasitic device capacitances result in higher absolute voltage slew rates during turn-on as well as turn off at increased DC-link voltage. Substrate configurations I and VIa, where the substrate is shorted and switched to source S_a respectively, exhibit almost identical switching transients. Marginally lower reduced voltage slew rate of VIa results from additional parasitic capacitances introduced by the active substrate switches T₁ and T_{II} (Fig. 8, solid black vs. solid green plot lines). In (semi-)floating substrate termination schemes II-V and VIb a transient bulk-source bias ($v_{BSa} \neq 0$ V) occurs during switching transitions. In combination with the non-linear parasitic bulk capacitances, the overall output capacitance of the bidirectional GaN HEMT is reduced which finally results in faster discharging of the switching node capacitance and therefore steeper voltage gradients during turn-on.

The ZVS turn-off transition of the bidirectional GaN HEMT T₂ is again directly correlated with a hard-switched turn-on of the unidirectional GaN HEMT T₁. The transient current peak (Fig. 8a, b right, $t=[5; 20]$ ns) is related to capacitive displacement currents as well as cross-conduction effects in the switching cell. Substrate configurations II-IV, where a significant positive bulk-source bias occurs, are correlated with a higher and/or longer transient current peak. Together with lower voltage slew rates dv_{SAs}/dt increased switching losses of the unidirectional GaN HEMT T₁ must be considered. In contrast, a slightly lower transient current peak is observed in substrate termination schemes V and VIb, where a

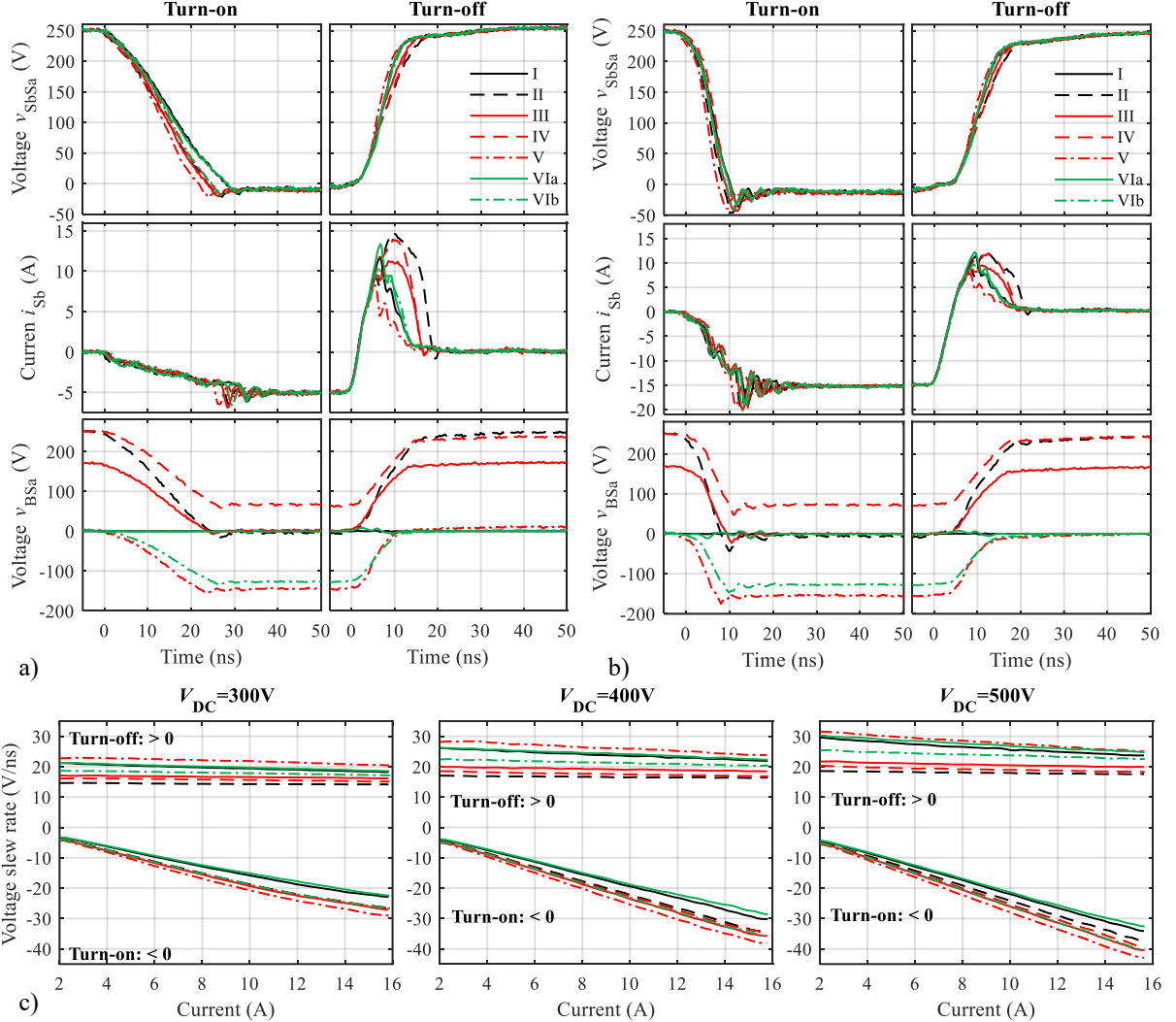


Fig. 8: Transient waveforms in soft-switched double-pulse test at $V_{DC}=500$ V and load currents of (a) $I_L=5$ A and (b) $I_L=15$ A and (c) average voltage slew rates (20%-80%)

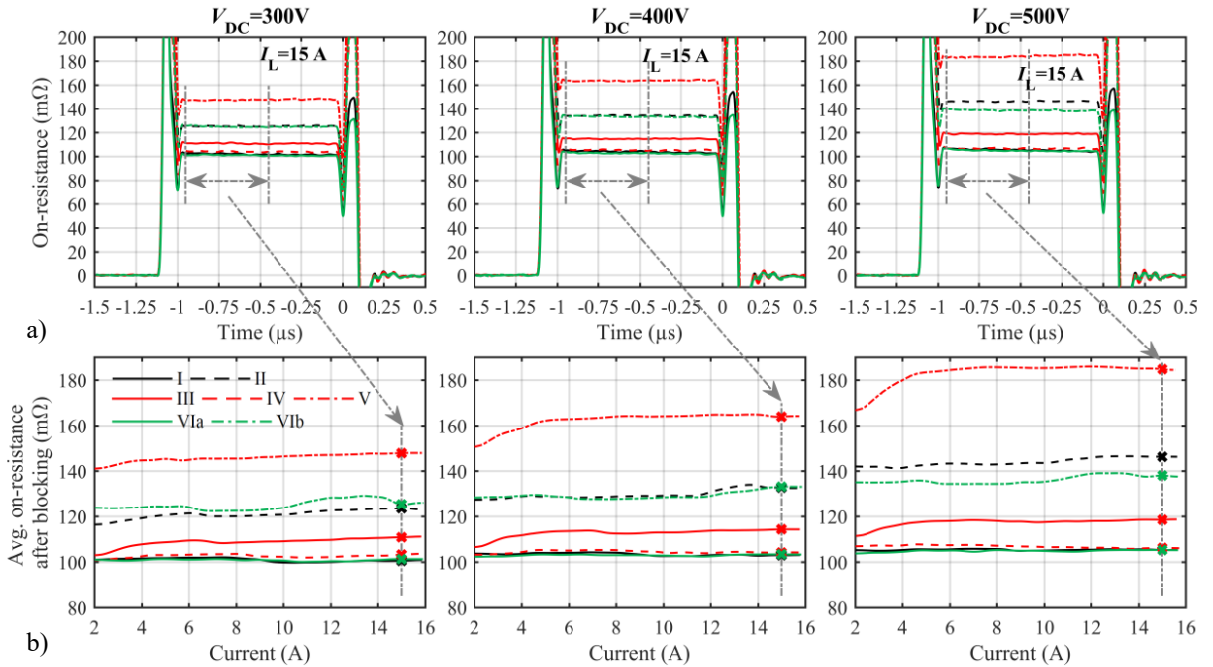


Fig. 9: Impact of the substrate termination on the (a) transient R_{ON} and (b) the average R_{ON} after blocking stress under soft-switched 3rd-quadrant ZVS conditions. Note that the transistor off-state drain bias is $V_{DC}/2$.

significant negative bulk-source bias occurs during on-state of the bidirectional transistor (Fig. 8a, b right, red and green dash-dot plot lines).

The transient R_{ON} in soft-switching double-pulse test is acquired during the 3rd-quadrant reverse conduction. In the timeframe of the preceding load inductor charging pulse the unidirectional GaN HEMT T₁ is conducting. Meanwhile the bidirectional GaN HEMT T₂ is exposed to off-state blocking stress and therefore prone to charge trapping causing dynamic R_{ON} -increase (Fig. 9). In soft-switching conditions the observed R_{ON} increases with the applied DC-link voltage (Fig. 9a). In comparison to hard-switched operation the absolute R_{ON} as well as its load-current dependency are notably reduced. The lowest R_{ON} is achieved using substrate terminations I and VIa, where a continuous substrate bias $v_{BSa} \approx 0$ V is guaranteed. Substrate termination IV exhibits a similar low R_{ON} (Fig. 9) although significant v_{BSa} -gradients occur during switching transitions while a positive bulk-source bias $v_{BSa} > 80$ V and $v_{BSa} > 250$ V is maintained during ON- and OFF-state respectively (Fig. 8a, b). The R_{ON} -degradation in soft-switching becomes especially extensive in configurations III, IV and VIb where a significant bulk-source bias gradient occurs combined with a temporarily bulk-source bias voltage which is close to zero or even negative (Fig. 8a and Fig. 9a).

4.4 Continuous operation in DC/DC buck-converter mode

The proposed active switched substrate termination scheme VIa has proven widely identical switching and dynamic on-state characteristics as a conventional fixed short of bulk and source (I) in both, hard- and soft-switched double-pulse characterization. The diode-based substrate termination scheme IV demonstrated similar on-state characteristics like configuration I and VIa at least under soft-switching conditions. Therefore, continuous operation measurements in DC/DC buck converter mode cover substrate termination schemes III, IV, VIa and VIb. The converter is operated in deep continuous conduction mode (CCM) and thermal steady state while a switching frequency $f_s = 50$ kHz, a duty cycle $D = 0.5$ and dead times $T_D = 80$ ns are applied. The employed PCB layout design is particularly optimized for minimum parasitic stray inductance and a small parasitic switching node capacitance while thermal design constraints are neglected. The maximum load current was limited to 6 A due to limited cooling capability of the PCB design. The bottom-side-cooled GaN HEMTs are exposed to forced air cooling. The T-type switching cell operation shows the highest efficiencies in both, hard- and soft-switching when using the active switches substrate termination scheme VIa, regardless of the DC-link voltage as well as load current (Fig. 10a vs. Fig. 11a). Other substrate termination schemes III, IV and VIb cause higher losses and device temperatures going along with reduced efficiency as well as lower maximum

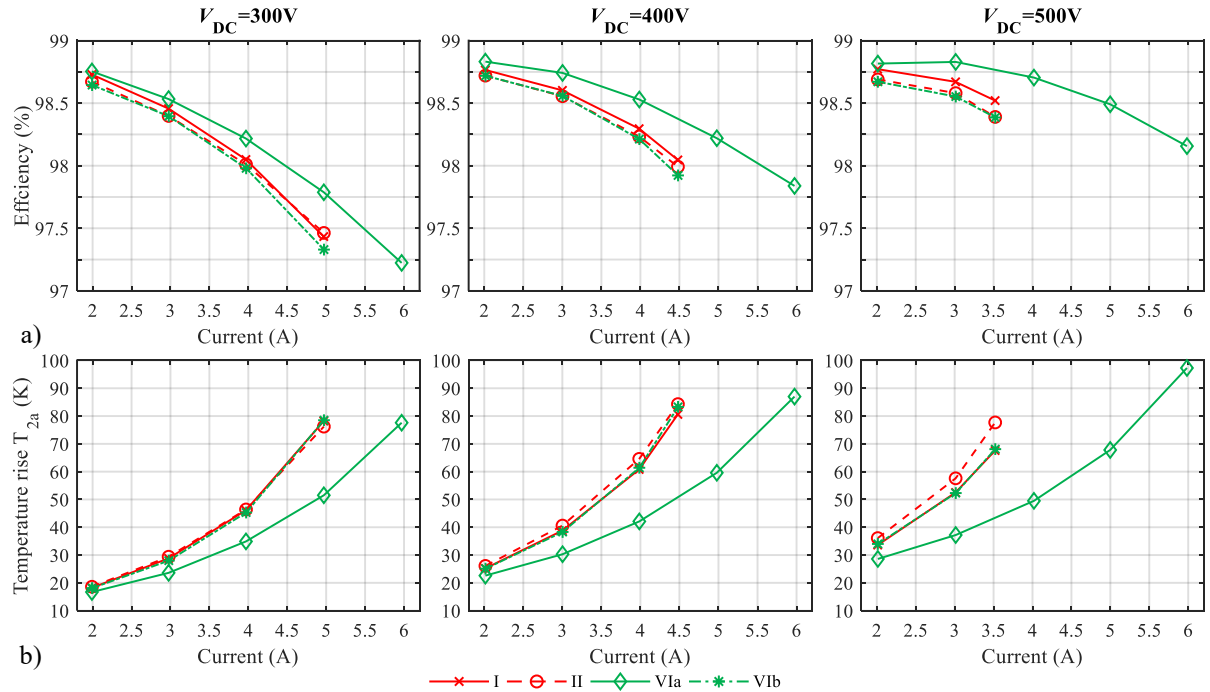


Fig. 10: Impact of the substrate termination on (a) the converter efficiency and (b) GaN HEMT package temperature rise vs. output current in hard-switched CCM DC/DC buck-converter operation

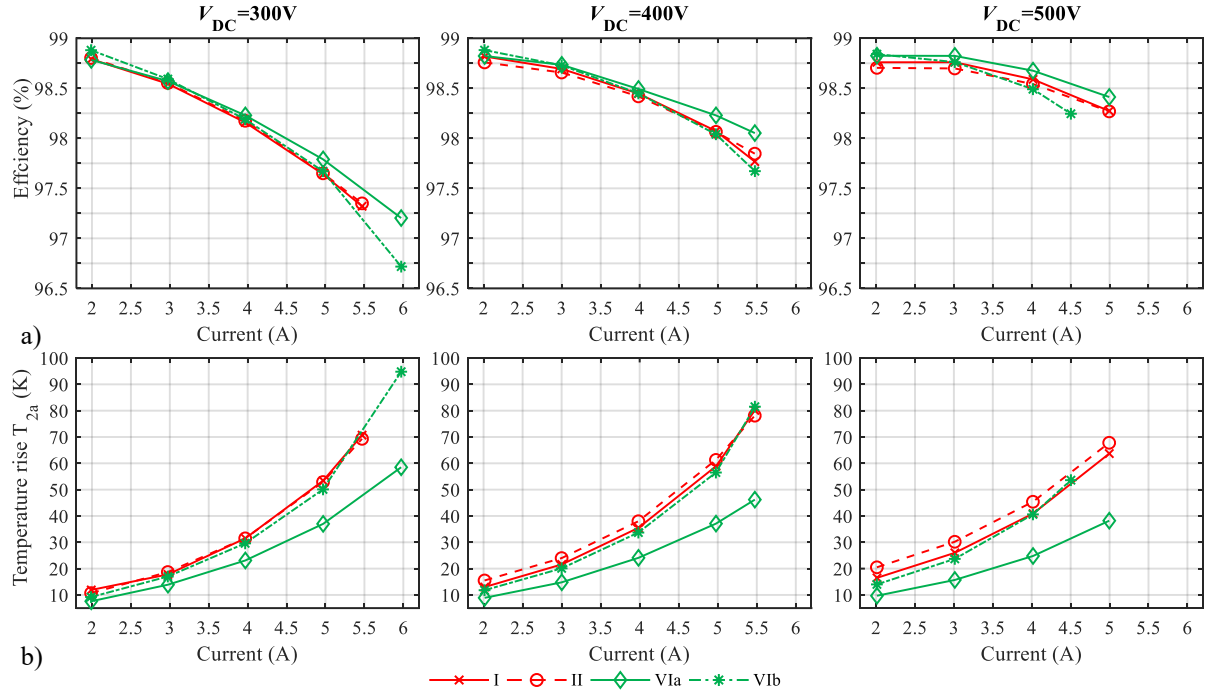


Fig. 11: Impact of the substrate termination on (a) the converter efficiency and (b) GaN HEMT package temperature rise vs. output current in soft-switched CCM DC/DC buck-converter operation

output currents. In agreement with the dynamic R_{ON} -characterization results in Sec. 4.2 and 4.3, the efficiency gains enabled by an active substrate termination are particularly pronounced in hard-switched operation. The significant impact on switching losses is further indicated when the temperature rises in Fig. 10 and Fig. 11 are compared. In 1st-quadrant hard-switching of the GaN HEMT T_{2a} which is part of the bidirectional transistor T_2 , the observed temperature rises are increased by up to 30 K in comparison to 3rd-quadrant ZVS operation when similar load conditions are considered (Fig. 10b vs. Fig. 11b).

Conclusion and future work

In this paper, different bidirectional switch implementations using lateral GaN HEMTs are presented. Monolithically integrated bidirectional GaN HEMTs with common drift region promise for significantly reduced R_{ON} compared to a discrete solution, but require a proper substrate termination preventing device degradation due to back-gating effects. Static and dynamic substrate coupling effects are studied for an electrically emulated monolithic bidirectional transistor which is based on discrete GaN-on-Si HEMTs. Several substrate termination schemes proposed before in literature are investigated with regard to their impact on switching and transient on-state characteristics in hard- and soft-switched operation of the device.

Based on the presented measurement results different degradation mechanisms due to substrate coupling are identified. Static device characteristics are degraded with respect to saturation current and R_{ON} when an increasingly negative substrate bias is applied, while a positive bias bulk-source voltage shows no effect. In contrast, in switched operation device degradation is mainly induced by gradients of the bulk-source bias and the related capacitive displacement currents occurring during switching transitions. An actively controlled substrate termination has demonstrated to overcome substrate coupling effects in switching tests of the emulated bidirectional GaN HEMT. Dynamic device characteristics in terms of switching speed and losses as well as the transient R_{ON} remain almost unaffected compared to a fixed substrate termination commonly used in unidirectional GaN HEMTs.

Efficiency measurements of the T-type switching cell in DC/DC operation with different substrate biasing configurations show the highest efficiencies for the proposed active substrate termination and thus support the findings from the static and switched device characterizations.

Future work will focus on the implementation and validation of the proposed active substrate termination in a monolithically integrated bidirectional GaN HEMT with common drift region in DC/AC operation of the T-type inverter. In addition, static and dynamic device degradation mechanisms will be analyzed by means of a physical transistor model.

References

- [1] C. Kuring, O. Hilt, J. Böcker, M. Wolf, S. Dieckerhoff und J. Würfl, „Novel monolithically integrated bidirectional GaN HEMT,“ in *2018 IEEE Energy Conversion Congress and Exposition (ECCE)*, 2018.
- [2] C. Kuring, N. Wieczorek, O. Hilt, M. Wolf, J. Böcker, J. Würfl und S. Dieckerhoff, „Impact of Substrate Termination on Dynamic On-State Characteristics of a Normally-off Monolithically Integrated Bidirectional GaN HEMT,“ in *2019 IEEE Energy Conversion Congress and Exposition (ECCE)*, 2019.
- [3] M. Wolf, O. Hilt und J. Würfl, „Gate Control Scheme of Monolithically Integrated Normally OFF Bidirectional 600-V GaN HFETs,“ *IEEE Transactions on Electron Devices*, Bd. 65, pp. 3878-3883, 2018.
- [4] EPC – Efficient Power Conversion Corporation, „eGaN® FET Datasheet EPC2110 – Dual Common-Source-Mode,“ 2017.
- [5] S. Léo, F. Jean-Paul, F. David, J. Pierre-Olivier, P. Pierre und L. Othman, „Implementation of monolithic bidirectional switches in a AC/DC Dual Active Bridge in ZVS auto-switching mode,“ in *2018 IEEE International Conference on Industrial Technology (ICIT)*, 2018.
- [6] Innoscience, „Datasheet 'INN40W08 - 40V Bi-GaN Enhancement-mode FET ',Rev.1.0 2021/11/26“.
- [7] „Datasheet 'GS66508P', Rev 190524“.
- [8] „Datasheet 'EPC2034C', revised June, 2020“.
- [9] H. Ueno, Y. Kinoshita, Y. Yamada, A. Suzuki, T. Ichiryu, M. Nomura, H. Fujiwara, H. Ishida und T. Hatsuda, „A 3-Phase T-type 3-Level Inverter using GaN Bidirectional Switch with Very Low On-State Resistance,“ in *PCIM Europe 2019; International Exhibition and Conference for Power Electronics, Intelligent Motion, Renewable Energy and Energy Management*, 2019.
- [10] F. Vollmaier, N. Nain, J. Huber, J. W. Kolar, K. K. Leong und B. Pandya, „Performance Evaluation of Future T-Type PFC Rectifier and Inverter Systems with Monolithic Bidirectional 600 V GaN Switches,“ in *2021 IEEE Energy Conversion Congress and Exposition (ECCE)*, 2021.
- [11] S. Bahl, M. Senesky, N. Tipirneni, D. Anderson und S. Pendharkar, "Bi-directional gallium nitride switch with self-managed substrate bias". Patent US20140374766A1 (20.06.2013).
- [12] M. Imam, H. Kim, K. Leong, B. Pandya und G. Prechtl, "Semiconductor device having a bidirectional switch and discharge circuit". US / EU Patent US20190326280A1 (23.04.2018) / EP3562040A1 (15.04.2019).
- [13] K. Leong, "Bidirectional switch with passive electrical network for substrate potential stabilization". Patent US10224924B1 (22.08.2017).
- [14] C. Kuring, M. Tannhaeuser und S. Dieckerhoff, „Improvements on Dynamic On-State Resistance in Normally-off GaN HEMTs,“ in *PCIM Europe 2019; International Exhibition and Conference for Power Electronics, Intelligent Motion, Renewable Energy and Energy Management*, 2019.
- [15] M. J. Uren, S. Karboyan, I. Chatterjee, A. Pooth, P. Moens, A. Banerjee und M. Kuball, „Leaky Dielectric“ Model for the Suppression of Dynamic R_{ON} in Carbon-Doped AlGaN/GaN HEMTs,“ *IEEE Transactions on Electron Devices*, Bd. 64, pp. 2826-2834, 2017.
- [16] B. Kohlhepp, C. Kuring, S. Peller und D. Kübrich, „Measurement of Dynamic On-State Resistance of High-Voltage GaN-HEMTs under Real Application Conditions,“ in *2020 22nd European Conference on Power Electronics and Applications (EPE'20 ECCE Europe)*, 2020.
- [17] A. Pozo, S. Zhang, G. Stecklein, RicardoGarcia, J. Glaser, Z. Tang, R. Strittmatter und A. Lidow, „GaN Reliability and Lifetime Projections,“ in *CIPS 2022; 12th International Conference on Integrated Power Electronics Systems*, 2022.